

Motion of Bound Domain Walls in a Spin Ladder

Indrani Bose *and Amit Kumar Pal

Department of Physics
Bose Institute
93/1 A. P. C. Road, Kolkata - 700009

Abstract

The elementary excitation spectrum of the spin- $\frac{1}{2}$ antiferromagnetic (AFM) Heisenberg chain is described in terms of a pair of freely propagating spinons. In the case of the Ising-like Heisenberg Hamiltonian spinons can be interpreted as domain walls (DWs) separating degenerate ground states. In dimension $d > 1$, the issue of spinons as elementary excitations is still unsettled. In this paper, we study two spin- $\frac{1}{2}$ AFM ladder models in which the individual chains are described by the Ising-like Heisenberg Hamiltonian. The rung exchange interactions are assumed to be pure Ising-type in one case and Ising-like Heisenberg in the other. Using the low-energy effective Hamiltonian approach in a perturbative formulation, we show that the spinons are coupled in bound pairs. In the first model, the bound pairs are delocalized due to a four-spin ring exchange term in the effective Hamiltonian. The appropriate dynamic structure factor is calculated and the associated lineshape is found to be almost symmetric in contrast to the 1d case. In the case of the second model, the bound pair of spinons lowers its kinetic energy by propagating between chains. The results obtained are consistent with recent theoretical studies and experimental observations on ladder-like materials.

1 Introduction

Low-dimensional quantum antiferromagnets exhibit a rich variety of phenomena indicative of novel ground and excited state properties [1, 2, 3]. In one dimension (1d), the ground and low-lying excited states of the spin chain, in which nearest neighbour spins of magnitude $\frac{1}{2}$ interact via the antiferromagnetic (AFM) Heisenberg exchange interaction, can be determined exactly using the Bethe Ansatz [4, 5]. The ground state has no long range order and the spin-spin correlations are characterized by a power-law decay. The elementary excitation is not the conventional spin-1 magnon but a pair of spin- $\frac{1}{2}$ excitations termed spinons. The physical origin of spinons can be best understood in the Ising limit of the exchange interaction Hamiltonian given by

$$H = \sum_{i=1}^N J_z S_i^z S_{i+1}^z + \sum_{i=1}^N \frac{J_{xy}}{2} (S_i^+ S_{i+1}^- + S_i^- S_{i+1}^+) \quad (1)$$

where S_i^\pm are the spin raising and lowering operators and N is the total number of spins. In the Ising limit ($J_{xy} = 0$), the ground states of the Hamiltonian are the doubly degenerate Néel states, one of which is shown in figure 1(a). An excited state is created by flipping a spin from its ground state arrangement, e.g., a down spin is flipped into an up spin in figure 1(b). The flip gives rise to two domain walls (DWs) consisting of parallel spins and shown by dotted lines in the figure [1, 6]. The transverse exchange interaction term in (1) interchanges the spins in an antiparallel spin pair and has the effect of making the DWs propagate independently (figure 1(c)). Since the original spin flip carries spin one, each of the DWs or spinons has spin- $\frac{1}{2}$ associated with it. Spinons are thus examples of fractional excitations in an interacting spin system.

Spinons can be detected through inelastic neutron scattering in which neutrons scatter against spins to create spin flips. Due to energy and momentum conservation, the energy absorption spectrum for spin flips at different wave vectors can be measured. One observes a peak at a well-defined energy if the spin flip creates a single particle excitation. In the case of a pair of spinons, the total energy ϵ and momentum k of the spin excitation are given by $\epsilon(k) = \epsilon_1(k_1) + \epsilon_2(k_2)$ and $k = k_1 + k_2$ where ϵ_i , k_i ($i = 1, 2$) denote individual spinon energy and momentum [1, 6]. The total momentum k of the spin flip can be

*indrani@bosemain.boseinst.ac.in

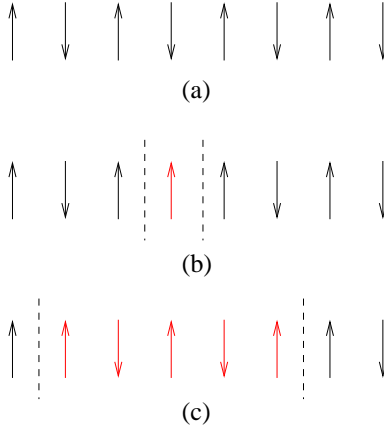


Figure 1: (a) Néel state, (b) a spin flip in the Néel state creates a pair of domain walls or spinons the locations of which are shown by dotted lines, (c) the transverse exchange interaction term in the Hamiltonian (equation (1)) gives rise to the propagation of independent spinons.

distributed in a continuum of ways among the spinons giving rise to a continuous absorption spectrum. For a single particle excitation, the energy versus momentum relation defines a single branch of excitations whereas for spinons a continuum of excitations with well-defined lower and upper boundaries is obtained. The compounds $CsCoCl_3$ and $CsCoBr_3$ are good examples of Ising-like Heisenberg antiferromagnets in 1d above the Néel temperature and provide evidence of the two-spinon continuum in neutron scattering experiments [6, 7, 8]. In the case of the isotropic Heisenberg Hamiltonian ($J_z = J_{xy}$ in equation (1)), the spinon spectrum has been clearly observed in the linear chain compound $KCuF_3$ [9] though a physical interpretation of spinons is not as straightforward as in the Ising-like case.

The existence of spinons, with fractional quantum number spin- $\frac{1}{2}$, is well established in 1d Heisenberg-type antiferromagnets. In higher dimensions, the spin-1 magnons are the elementary excitations in magnetically ordered ground states. There are theoretical suggestions that quantum antiferromagnets with spin-liquid (no magnetic long range order and without broken symmetry) ground states may support elementary spinon-like excitations with fractional quantum numbers [10, 11, 12]. A well-known example is that of a resonating-valance-bond (RVB) state, a linear superposition of VB states, in which the spins are paired in singlet (VB) configurations. A broken VB gives rise to a pair of free spins which may propagate independently to give rise to spinon excitations. If the energetic cost of deconfinement is high, the spinons propagate as a bound pair (confinement) so that the elementary excitation has spin-1.

Despite considerable effort, there are few experimental evidences of spinon-like excitations in $d > 1$ [13, 14]. One strong candidate is Cs_2CuCl_4 , a spin- $\frac{1}{2}$ Heisenberg antiferromagnet defined on a spatially anisotropic triangular lattice [13]. The dynamical structure factor $S(k, \omega)$ for Cs_2CuCl_4 , where k and ω are the momentum and energy transfers in the neutron scattering experiment, is dominated by a broad continuum which has been cited as evidence for fractionalized excitations. Kohno et al [15] reanalyzed the neutron scattering data to show that the spinons are not characteristic of some exotic 2d state but are descendants of the weakly-coupled excitations of individual chains in the material. The spectrum also has a sharp dispersing peak attributed to ‘triplon’ bound states of the spinons. The bound pair lowers its kinetic energy through propagation between chains. The issue of fractional versus integer excitations has been extensively investigated in AFM spin- $\frac{1}{2}$ ladders [16, 17, 18, 19, 20]. A two-chain ladder consists of two AFM chains coupled by rung exchange interactions. The spinons of individual chains are confined even if the rung exchange interaction strength is infinitesimal. Ladders with strong rung exchange couplings suppress spinon excitations at all energy scales. Recently, Lake et al [21] have carried out neutron scattering experiments on a weakly-coupled ladder material, $CaCu_2O_3$, and shown that deconfined spinons at high energies evolve into $S = 1$ excitations at lower energies. The spinons are associated with individual chains whereas the $S = 1$ excitations are the triplon excitations, i.e., bound states of spinons. Two approaches are usually adopted in probing the nature of excitations in spin ladders: (i) the rung coupling strength dominates and (ii) the rung coupling strength is weaker than the intra-chain coupling strengths [21]. In this paper, we consider a different case, not studied earlier, in which two $S = \frac{1}{2}$ Ising-like Heisenberg AFM chains, each of which is described by a Hamiltonian of the type shown in equation (1), are coupled by Ising or Ising-like Heisenberg AFM exchange interactions. In section II, we investigate the nature of the low-lying excitations with Ising rung exchange interactions. In section III, the rung exchange interactions are considered to be Ising-like Heisenberg AFM in nature. Section IV contains concluding remarks.

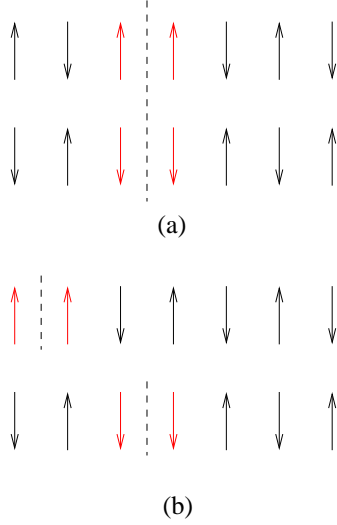


Figure 2: (a) A pair of DWs in the minimum energy configuration of a ladder with an odd number N of rungs. (b) Motion of the DW in the top chain leaves in its wake ferromagnetically aligned rung spins which raises the energy of the system.

2 Ising Rung Exchange Interactions

We consider an antiferromagnetic two-chain spin ladder with the spins of magnitude $\frac{1}{2}$. The individual chains of the ladder are described by the Ising-Heisenberg Hamiltonian (equation(1)). The chains are coupled by rungs with the corresponding exchange interactions being of the Ising-type. The ladder Hamiltonian H_L is given by

$$\begin{aligned}
 H_L &= J_Z \sum_{\alpha=1}^2 \sum_{i=1}^N S_{i,\alpha}^Z S_{i+1,\alpha}^Z + J_Z \sum_{i=1}^N S_{i,1}^Z S_{i,2}^Z + \frac{J_{XY}}{2} \sum_{\alpha=1}^2 \sum_{i=1}^N (S_{i,\alpha}^+ S_{i+1,\alpha}^- + S_{i,\alpha}^- S_{i+1,\alpha}^+) \\
 &= H_Z + H_{XY}
 \end{aligned} \tag{2}$$

where the index $\alpha = 1(2)$ refers to the top (bottom) chain of the ladder, i denotes the site index and N is the total number of rungs. We also assume that the anisotropy constant $\epsilon = \frac{J_{XY}}{J_Z}$ is $\ll 1$. Hence, the Ising part of the Hamiltonian, H_Z , can be considered to be the unperturbed Hamiltonian with H_{XY} , containing the transverse exchange interactions, providing the perturbation. Since H_Z is AFM in nature, the lowest energy states are the Néel states with n.n. spin pairs antiparallel. In the spirit of Villain [6], we first consider a ladder with an odd number of rungs, i. e., $N = \text{odd}$ and periodic boundary conditions (PBCs). Energies are measured w. r. t. that of a Néel configuration of spins. Since there are $3N$ n.n. spin pairs, the energy of a configuration in which all such pairs are antiparallel is $E_{\text{Néel}} = -3N \frac{J_Z}{4}$. Since N is odd, a perfect Néel configuration is not possible and the lowest energy states of H_Z contain a pair of parallel spin pairs which define the DWs or spinons (figure 2 (a)). The DWs form a bound pair to ensure minimal energy loss. Any other arrangement of DWs in the individual chains gives rise to higher energy states. The lowest energy states are N -fold degenerate as there are N possibilities for the location of the bound pair which is an $S_z = 0$ object.

We next consider the effect of the perturbing Hamiltonian on the minimum energy states. The transverse exchange interaction can give rise to independent DW motion in the chains which, however, costs energy as a propagating DW leaves in its wake ferromagnetically aligned rung spins (figure 2(b)). The energy cost increases as the distance between the DWs increases resulting in confinement of the DW pair. We investigate the dynamics of the DW pair perturbatively using a low-energy effective Hamiltonian (LEH) [22, 23]. The N -fold degenerate DW pair states $|p_i\rangle$, $i = 1, \dots, N$ (figure 2(a)) constitute the low-energy manifold and have energy $E_0 = -\frac{3NJ_Z}{4} + J_Z$. The higher energy states of H_Z are denoted by $|q_\alpha\rangle$ with energy E_α . The perturbing Hamiltonian H_{XY} connects the low-energy manifold to the manifold of higher-energy states. In general, perturbation lifts the degeneracy of the low-energy manifold leading to an effective Hamiltonian operating in the space of states associated with the low-energy manifold. Diagonalization of the n -th order ($n = 1, 2, \dots$) effective Hamiltonian in the low-energy subspace of states reproduces the n -th order energy corrections to the low-energy unperturbed states. Using degenerate perturbation theory, the first order LEH is given, up to an overall constant, by [23]

$$H_{eff}^{(1)} = \sum_{ij} |p_i\rangle \langle p_i| H_{XY} |p_j\rangle \langle p_j| \tag{3}$$

$$H_{XY} \left| \begin{array}{cccccc} \uparrow & \downarrow & \uparrow & \downarrow & \uparrow & \downarrow \\ \downarrow & \uparrow & \downarrow & \uparrow & \downarrow & \uparrow \end{array} \right\rangle = \frac{J_{XY}}{2} |q_1\rangle$$

$$H_{XY} |q_1\rangle = \frac{J_{XY}}{2} \left| \begin{array}{cccccc} \uparrow & \downarrow & \uparrow & \downarrow & \uparrow & \downarrow \\ \downarrow & \uparrow & \downarrow & \uparrow & \downarrow & \uparrow \end{array} \right\rangle$$

Figure 3: Two successive applications of H_{XY} on low-energy states shifts the location of the bound DW pair by two lattice constants.

The second-order LEH has the form

$$H_{eff}^{(2)} = \sum_{ij} \sum_{\alpha} |p_i\rangle \frac{\langle p_i | H_{XY} | q_{\alpha} \rangle \langle q_{\alpha} | H_{XY} | p_j \rangle}{E_0 - E_{\alpha}} \langle p_j | \quad (4)$$

Since the matrix element $\langle p_i | H_{XY} | p_j \rangle = 0$, the LEH is determined using the second-order expression in equation (4). Two types of processes contribute to $H_{eff}^{(2)}$. In “diagonal” processes, the spins in an antiparallel pair exchange and then reexchange back to the original configuration ($|p_i\rangle = |p_j\rangle$). Such processes do not lift the degeneracy and give rise to a constant energy shift. We neglect this contribution in deriving the effective Hamiltonian. In the off-diagonal processes, the spins in two antiparallel pairs belonging to the four-spin plaquettes bordering the bound DW pair are interchanged. For the DW pair state shown in figure 2(a), the intermediate states $|q_i\rangle$, $i = 1, \dots, 4$ are given by

$$\begin{aligned} |q_1\rangle &= \begin{array}{cccccc} \uparrow & \uparrow & \downarrow & \uparrow & \downarrow & \uparrow & \downarrow \\ \downarrow & \uparrow & \downarrow & \downarrow & \uparrow & \downarrow & \uparrow \end{array} \\ |q_2\rangle &= \begin{array}{cccccc} \uparrow & \downarrow & \uparrow & \uparrow & \downarrow & \uparrow & \downarrow \\ \downarrow & \downarrow & \uparrow & \downarrow & \uparrow & \downarrow & \uparrow \end{array} \\ |q_3\rangle &= \begin{array}{cccccc} \uparrow & \downarrow & \uparrow & \downarrow & \uparrow & \uparrow & \downarrow \\ \downarrow & \uparrow & \downarrow & \downarrow & \uparrow & \downarrow & \downarrow \end{array} \\ |q_4\rangle &= \begin{array}{cccccc} \uparrow & \downarrow & \uparrow & \uparrow & \downarrow & \uparrow & \downarrow \\ \downarrow & \uparrow & \downarrow & \uparrow & \downarrow & \downarrow & \uparrow \end{array} \end{aligned} \quad (5)$$

The spin pairs deviated from the arrangement shown in figure 2 (a) are marked by double arrows. The perturbing Hamiltonian, H_{XY} , acting on the intermediate $|q_{\alpha}\rangle$ states shifts the location of the bound DW pair by two lattice constants either towards the left or the right. This is illustrated in figure 3 for the state $|q_1\rangle$. The energy of the states $|q_{\alpha}\rangle$ ($\alpha = 1, \dots, 4$) is $E_{\alpha} = -\frac{3NJ_Z}{4} + 2J_Z$. The second-order LEH is thus given by

$$H_{eff}^{(2)} = -\frac{\epsilon^2 J_Z}{2} \sum_i (|p_{i+2}\rangle \langle p_i| + |p_{i-2}\rangle \langle p_i|) \quad (6)$$

where $\epsilon = \frac{J_{XY}}{J_Z}$. The off-diagonal processes are equivalent to “ring” exchanges involving four spins. The full second-order Hamiltonian, defined in the low-energy manifold, is thus given by

$$H_{eff} = H_Z + H_{ring} \quad (7)$$

where

$$H_{ring} = J_{ring} \sum_{\square} (S_1^+ S_2^- S_3^+ S_4^- + h.c.) \quad (8)$$

with $J_{ring} = -\frac{\epsilon^2 J_Z}{2}$ and the sum over all elementary plaquettes of the ladder. Ring or cyclic exchange interactions (equation (8)) also appear in the perturbative effective Hamiltonian theories developed for the XXZ Heisenberg model on the checkerboard lattice [24] and in the case of an easy-axis Kagomé antiferromagnet [25]. In the ladder model, the ring exchange interaction has the effect of deconfining the bound DW pair. In the low-energy subspace, the dispersion relation of the bound pair can be determined in a straightforward manner. The eigenstate $\psi(k)$ of the pair can be written as a linear combination of states $|j\rangle$ ($j = 1, 2, \dots, N$) where j denotes the location of the bound DW pair.

$$|\psi(k)\rangle = \frac{1}{\sqrt{N}} \sum_{j=1}^N e^{ikj} |j\rangle \quad (9)$$

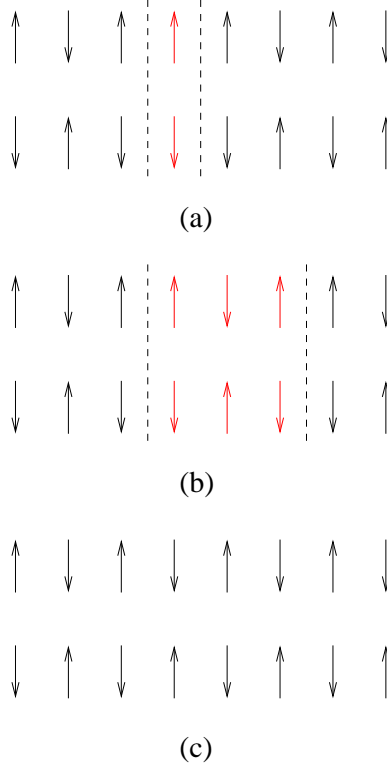


Figure 4: Bound DW pair states for (a) $\mu = 1$ and (b) $\mu = 3$. The dotted lines indicate the locations of the bound DW pairs; (c) One of the ground states, $\psi_{Néel1}$, of H_Z .

H_{eff} (equation (7)) operating on $|\psi(k)\rangle$ yields the eigenvalue

$$\omega_b(k) = J_Z(1 - \epsilon^2 \cos 2k) \quad (10)$$

The subscript ‘b’ in ω_b denotes that the dispersion relation is that of a bound DW pair.

We next consider a two-chain spin ladder with an even number N of rungs and described by the Hamiltonian in equation (7) satisfying PBCs. The low-lying excitation spectrum is obtained in the subspace of degenerate eigenstates of H_Z which are generated by flipping all the spins in a block of μ (μ may be odd/even) adjacent rungs in the ground state (Néel state) of H_Z . Each of the states contains two bound DW pairs (figure 4) and has energy

$$E_{DW} = -\frac{3NJ_Z}{4} + 2J_Z \quad (11)$$

The z -component of the total spin of each state, $S_z^{tot} = 0$. We consider μ to be odd with the degenerate eigenstates of H_Z given by

$$\begin{aligned} \psi_1(k) &= \sqrt{\frac{2}{N}} \sum_j e^{ikj} \mathcal{S}_j \psi_{Néel1} \\ \psi_3(k) &= \sqrt{\frac{2}{N}} \sum_j e^{ikj} \mathcal{S}_j \mathcal{S}'_{j+1} \mathcal{S}_{j+2} \psi_{Néel1} \\ &\dots \\ \psi_{N-1}(k) &= \sqrt{\frac{2}{N}} \sum_j e^{ikj} \mathcal{S}_j \Pi_{\mu=1}^{\frac{N}{2}-1} \mathcal{S}'_{j+2\mu-1} \mathcal{S}_{j+2\mu} \psi_{Néel1} \end{aligned} \quad (12)$$

where $\mathcal{S}_k = S_{k,1}^+ S_{k,2}^-$ and $\mathcal{S}'_k = S_{k,1}^- S_{k,2}^+$. $\psi_{Néel1}$ is the ground state of H_Z shown in figure 4(c). The Hamiltonian H_{ring} in (7) has the following matrix elements between the Ising eigenstates :

$$\langle \psi_1(k) | H_{ring} | \psi_3(k) \rangle = \langle \psi_3(k) | H_{ring} | \psi_5(k) \rangle = \dots = J_{ring} (1 + e^{-2ik}) \equiv v \quad (13)$$

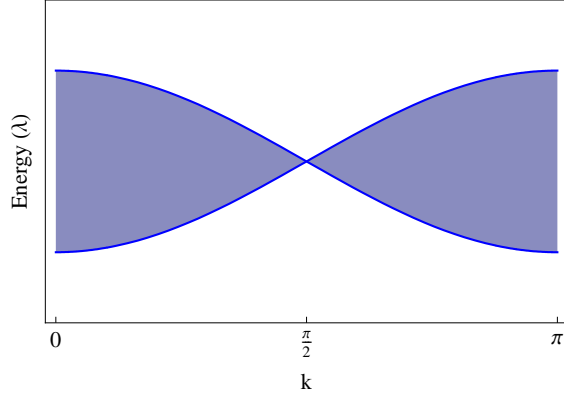


Figure 5: Excitation continuum with energies given in equation (17) and $\epsilon = 0.15$

where $J_{ring} = -\frac{\epsilon^2 J_Z}{2}$. The low-lying excited state of the Hamiltonian H_{eff} (equation (7)) is given by

$$\psi_{DW}(k) = \sum_{\nu=1}^{N/2} C_{\nu} \psi_{2\nu-1}(k) \quad (14)$$

From the eigenvalue equation $H_{eff}\psi_{DW}(k) = \lambda\psi_{DW}(k)$, one obtains

$$\sum_{\nu'=1}^{N/2} \langle \nu | H_{eff} | \nu' \rangle C_{\nu'} = \lambda C_{\nu} \quad (15)$$

where

$$\begin{aligned} \langle \nu | H_{eff} | \nu' \rangle &= 2J_Z \text{ for } \nu' = \nu \\ &= v \text{ for } \nu' = \nu + 1 \\ &= v^* \text{ for } \nu' = \nu - 1 \\ &= 0 \text{ otherwise} \end{aligned} \quad (16)$$

The diagonal matrix element is $2J_Z$ as energies are measured with respect to the Néel state energy $-\frac{3NJ_Z}{4}$ (see equation (11)). We choose the coefficients C_{ν} 's to be $C_{\nu} = e^{-i\phi\nu}$. The eigenvalues constitute an excitation continuum given by

$$\lambda = 2J_Z [1 - \epsilon^2 \cos k \cos(k + \phi)] \quad (17)$$

where $-\pi < \phi \leq \pi$.

Figure 5 shows the excitation continuum with upper and lower bounds given by $2J_Z(1 \pm \epsilon^2 \cos k)$. The degenerate eigenstates of H_Z defined in (12) correspond to the top chain of the spin ladder being in as $S_{tot,1}^z = +1$ and the bottom chain being in an $S_{tot,2}^z = -1$ state. One can construct a set of degenerate eigenstates with the situation reversed. Also, μ , the number of adjacent rungs constituting the block of flipped spins can be even ($\mu = 2, 4, 6, \dots$). There are two distinct sets of such states [8, 26]. All these subspaces of states give rise to the same excitation continuum (figure 5). The excitation continuum arises due to the motion of two walls each of which consists of a bound pair of DWs.

One notes that the effects of H_{ring} , for the two-chain ladder, and H_{XY} , for the 1d chain, on the DW states are similar. In the first case, a bound pair of DWs shifts by two lattice constants and in the second case a single DW shifts by the same distance. In the case of a single chain, the eigenvalues λ_{1d} constituting the excitation continuum are

$$\lambda_{1d} = J_Z [1 + 2\epsilon \cos k \cos(k + \phi)] \quad (18)$$

Comparing equations (17) and (18), one finds that the spread of the continuum around the unperturbed level is less in the case of the spin ladder.

The dynamic form factor, $S_{11}(q, \omega)$, associated with the bound DW pair is defined at $T = 0$ by

$$S_{11}(q, \omega) = \sum_f |\langle f | A(q) | g \rangle|^2 \delta(\omega - E_f + E_g) \quad (19)$$

where

$$A(q) = \frac{1}{\sqrt{N}} \sum_l A_l e^{iq l} A_l = (S_{i,1}^+ S_{i,2}^- + S_{i,1}^- S_{i,2}^+) \quad (20)$$

In (19), $|g\rangle$ and $|f\rangle$ are the ground and excited states of H_{eff} connected by $A(q)$, with energies E_g and E_f respectively, ω and q are the frequency and wave number of the excitation. $S_{11}(q, \omega)$, involving a pair of spin deviations, could be probed by the light-scattering techniques [27, 28]. Upto the first order of J_{ring} ($J_{ring} \ll J_Z$ in (7)),

$$|g\rangle \simeq \psi_{N\acute{e}el1} + \frac{1}{E_0 - H_Z} H_{ring} \psi_{N\acute{e}el1} \quad (21)$$

where E_0 is the energy of $\psi_{N\acute{e}el1}$. Since H_{ring} acting on $\psi_{N\acute{e}el1}$ creates two bound DW pairs, $\frac{1}{E_0 - H_Z} = -\frac{1}{2J_Z}$. Thus,

$$A(q)|g\rangle \simeq \frac{1}{\sqrt{2}} \left(1 + \frac{\epsilon^2}{2} \cos q \right) \psi_1(q) + \frac{1}{\sqrt{2}} \frac{v^*}{-2J_Z} \psi_3(q) \quad (22)$$

where $\psi_1(q)$ and $\psi_3(q)$ are as defined in equation (12) and $v^* = -\frac{\epsilon^2 J_Z}{2} (1 + e^{2iq})$. Using equation (22) and (19) and the expression (14) for $|f\rangle = \psi_{DW}(k)$, one gets following the procedures described in [7, 26]

$$\begin{aligned} S_{11}(q, \omega) &\simeq \frac{\sqrt{4|v|^2 - \Omega^2}}{2\pi|v|^2} \left(1 + \epsilon^2 \cos q - \frac{\Omega}{J_Z} \right) \text{for } |\Omega| < 2|v| \\ &= 0 \text{ otherwise} \end{aligned} \quad (23)$$

with $\Omega = \omega - 2J_Z$.

The expression (23) is similar to that for the dynamic structure factor $S_{xx}(q, \omega)$ of the 1d chain obtained in first order perturbation theory [7] ($A_l = S_l^x$ in equation (20)) except that in the latter case, $\Omega = \omega - J_Z$ and the contribution of the anisotropy term is to first order in ϵ . Figure 6 shows the plots of $S_{11}(q, \omega) \times 2J_Z |\cos q|$ versus $\frac{\omega}{J_Z}$ for $\epsilon = 0.15$ and for various values of the wave number q . The lineshape is almost symmetric in contrast to the prominent asymmetry found in the 1d case [7].

3 Ising-Heisenberg Rung Exchange Interactions

We now consider the case in which the rung exchange interactions of the two-chain spin ladder are Ising-like Heisenberg-type. The Hamiltonian is given by

$$\begin{aligned} H_R &= J_Z \sum_{\alpha=1}^2 \sum_{i=1}^N S_{i,\alpha}^z S_{i+1,\alpha}^z + J_Z \sum_{i=1}^N S_{i,1}^z S_{i,2}^z + \frac{J_{XY}}{2} \sum_{\alpha=1}^2 \sum_{i=1}^N (S_{i,\alpha}^+ S_{i+1,\alpha}^- + S_{i,\alpha}^- S_{i+1,\alpha}^+) \\ &\quad + \frac{J_{XY}}{2} \sum_{i=1}^N (S_{i,1}^+ S_{i,2}^- + S_{i,1}^- S_{i,2}^+) \\ &= H_Z + H_{XY} \end{aligned} \quad (24)$$

The Hamiltonian (24) differs from H_L in equation (2) by the addition of the last term. The ground states of H_Z are the doubly degenerate Néel states. We consider the Néel state $\psi_{N\acute{e}el1}$ shown in figure 4(c). The ladder can be divided into two sublattices A and B such that in $\psi_{N\acute{e}el1}$ the $A(B)$ sublattice spins are pointing up (down). The ground state energy $E_0 = -\frac{3NJ_Z}{4}$.

The lowest energy excitation of the unperturbed Hamiltonian is obtained by flipping a single spin in either the A ($S_{tot}^z = -1$) or the B ($S_{tot}^z = +1$) sublattice. We consider the latter case with $|i\rangle$ denoting the state in which the flipped spin is located in the i th rung (figure 7(a)). These excited states are N -fold degenerate with the energy

$$E_1 = -\frac{3NJ_Z}{4} + \frac{3J_Z}{2} \quad (25)$$

The perturbing Hamiltonian acting on the state $|i\rangle$ generates the following states

$$H_{XY}|i\rangle = \frac{\epsilon J_Z}{2} [|1\rangle + |2\rangle + |3\rangle + |4\rangle + \dots] \quad (26)$$

where $\epsilon = \frac{J_{XY}}{J_Z}$. The states $|m\rangle$ ($m = 1, \dots, 4$) are shown in figure 7(b) with energy

$$E_m = -\frac{3NJ_Z}{4} + \frac{5J_Z}{2} \quad (27)$$

The other states which are generated when H_{XY} acts on the state $|i\rangle$ have higher energies and are hence not considered. H_{XY} acting on the states $|m\rangle$ gives

$$\begin{aligned} H_{XY}|m\rangle &= \frac{\epsilon J_Z}{2} (|i\rangle + |i-1\rangle), \quad m = 1, 2 \\ &= \frac{\epsilon J_Z}{2} (|i\rangle + |i+1\rangle), \quad m = 3, 4 \end{aligned} \quad (28)$$

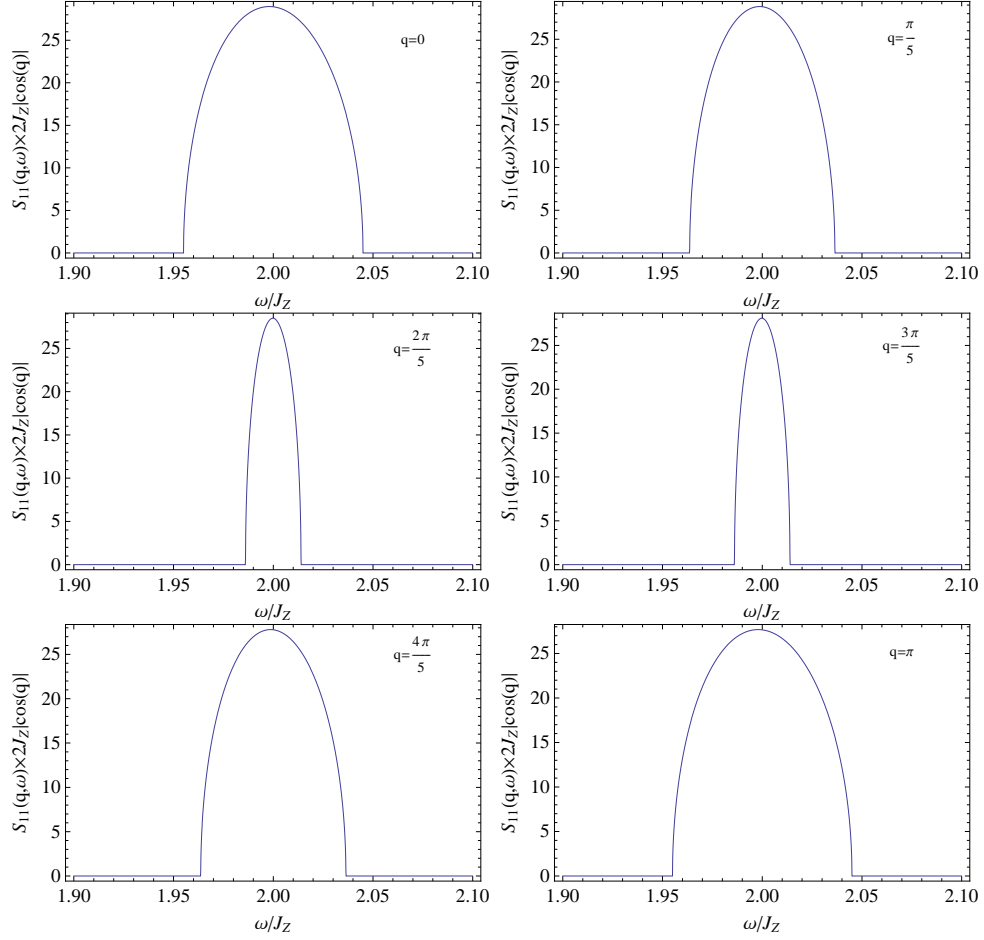


Figure 6: $S_{11}(q, \omega) \times 2J_Z |\cos q|$ evaluated in second-order perturbation theory for $\epsilon = 0.15$ versus $\frac{\omega}{J_Z}$ for different values of q .

In first order perturbation theory there is no energy correction. A finite energy correction is obtained in the second order perturbation theory. The effective LEH (equation (4)) with $|p_i\rangle = |i\rangle$, $|p_j\rangle = |j\rangle$, $|q_\alpha\rangle = |m\rangle$ and $E_\alpha = E_m$ in the same order is given by

$$H_{eff1}^{(2)} = -\frac{\epsilon^2 J_Z}{2} \sum_i (|i\rangle\langle i-1| + |i\rangle\langle i+1|) \quad (29)$$

$$= -\frac{\epsilon^2 J_Z}{2} \sum_{i=1}^N \sum_{\delta=-1,1} (S_{i,1}^+ S_{i+\delta,2}^- + S_{i,1}^- S_{i+\delta,2}^+) \quad (30)$$

The effect of this Hamiltonian on the low-energy excited state $|i\rangle$ (figure 7(a)) is to shift the flipped spin from the i th to the $(i+1)$ th or the $(i-1)$ th rungs. Since the flipped spins are located in the B sublattice, the shift is in the diagonal direction. The flipped spin is associated with a bound pair of DWs in a chain. The bound pair lowers its kinetic energy by propagating between chains. The full second-order Hamiltonian defined in the low-energy manifold of states with single spin flips, is

$$H_{eff1} = H_Z + H_{eff1}^{(2)} \quad (31)$$

As before, we have not included the terms arising from the “diagonal” processes in equation (4) as they give rise to a constant energy shift. The low energy excited state with $S_{tot}^z = +1$ can be constructed as

$$|k\rangle = \frac{1}{\sqrt{N}} \sum_{j=1}^N e^{ikj} S_{j,B}^+ |\psi_{N\epsilon\ell 1}\rangle \quad (32)$$

where ‘ B ’ denotes the B sublattice. The dispersion relation for the propagation of the flipped spin or equivalently the bound DW pair is given by

$$E_1(k) = J_Z (1 - \epsilon^2 \cos k) \quad (33)$$

where the energy is measured w. r. t the Néel state energy. The bound DW pair moves diagonally across the spin ladder. The unperturbed Hamiltonian, H_Z , is the same irrespective of whether the rung exchange interactions are Ising-type or Ising-Heisenberg-type. Thus, the lowest unperturbed excited state is the single flip state in both the cases. The excitation has a localized character when the rung exchange interactions are of the Ising-type. The bound DW pair associated with the single spin-flip can not propagate between the chains as the inter-chain interactions are Ising-like and propagation of the DWs in a single chain is, as pointed out before, energetically prohibitive. The energy, $-\frac{3J_Z}{2}$, of the localized excitation is lower than that of the propagating excitations involving two bound DW pairs when the rung exchange interactions are of the Ising-type (section 2). In this case, propagating excitations with the lowest energy involve two bound DW pairs rather than one.

4 Concluding Remarks

AFM spin models in which the existence of spinons is well-established include the spin- $\frac{1}{2}$ Heisenberg AFM chain [1], the Majumdar-Ghosh model [29] and the Haldane-Shastry model [30, 31]. The physical picture of a spinon as a DW between two degenerate ground states emerges in the Ising-Heisenberg limit of the AFM Hamiltonian [1, 7, 8]. In the case of the MG model, the spin- $\frac{1}{2}$ excitation acts as a DW between the two dimerized ground states of the model [32, 33]. In a closed chain, the DWs occur in pairs so that the lowest-lying excitation is given by the two-spinon continuum. The spinons are deconfined in this case and can move away from each other. There is no energy cost in moving the spinons far apart. This is not so when two AFM chains are coupled in the form of a spin ladder. Let J_\perp and J_\parallel be the strengths of the rung and intra-chain n.n. exchange interactions respectively. The spinon excitations of individual chains are confined by even an infinitesimal coupling strength J_\perp [18, 21]. The two $S = \frac{1}{2}$ spinons form a bound state giving rise to singlet and triplet excitation branches. In the case of the strongly coupled ladder ($J_\perp \gg J_\parallel$), the elementary excitation is a triplet. Lake et al. [21] carried out neutron scattering experiments on the weakly-coupled ($J_\perp \ll J_\parallel$) ladder material CaCu_2O_3 and obtained evidence of the singlet excitation mode. The spinon continuum was observed at high energies for which the chains are effectively decoupled. The spinons in a chain evolve into an $S = 1$ excitation at lower energies thereby confirming that the $S = 1$ “triplon” excitation is a bound state of two spinons and not a conventional magnon.

In this paper, we study a two-chain $S = \frac{1}{2}$ AFM spin ladder in which the individual chains are described by the Ising-like Heisenberg Hamiltonian and the rung couplings are of the Ising-type. Using a low-energy effective Hamiltonian approach, we establish that in a ladder with an odd number of rungs the spinons (DWs) form a bound pair. A four-spin ring exchange interaction in the effective Hamiltonian is responsible for the delocalization of the bound pair. In the case of a ladder with an even number of rungs, the low-lying propagating excitation involves two bound pairs of DWs which can move away from each other giving rise to a continuum of excitations. The physical origin of the excitation continuum is similar to that in the case of the Ising-Heisenberg AFM chain in 1d except that in the former case the spinons form bound pairs and the dispersion

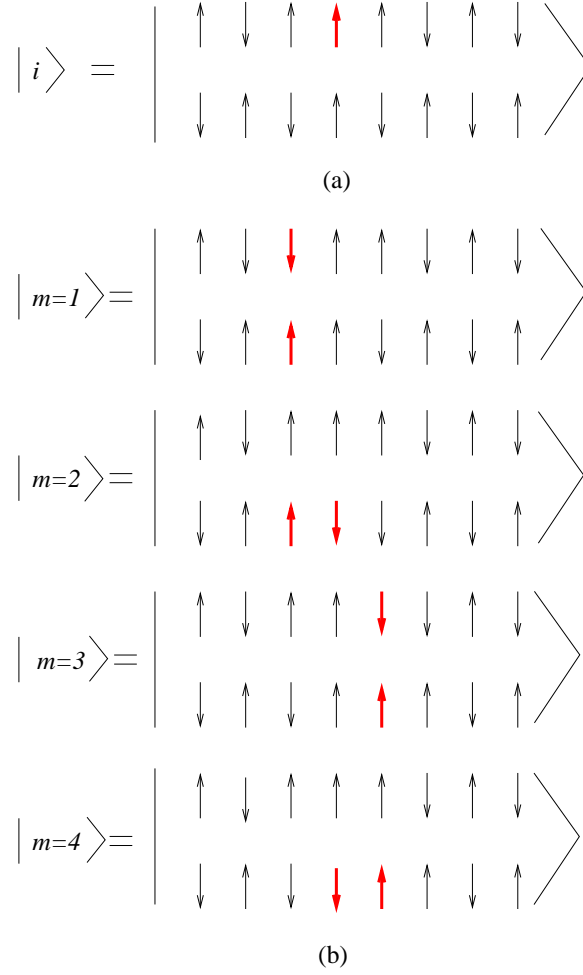


Figure 7: (a) The lowest energy excitation ($S_{tot}^z = +1$) of the unperturbed Hamiltonian H_Z in equation (24). The deviated spin is represented by a thick arrow. (b) The perturbing Hamiltonian, H_{XY} , acting on the state $|i\rangle$ generates the states $|m\rangle (m = 1, 2, 3, 4)$. The spin deviations from the state $|i\rangle$ are shown by thick arrows.

of the excitation spectrum is a higher-order effect in perturbation theory. This results in an almost symmetric lineshape in the case of the dynamic structure factor $S_{11}(q, \omega)$ (Figure 6) in contrast to the asymmetry observed in the structure factor $S_{xx}(q, \omega)$ in 1d [7]. The delocalization of a bound spinon pair is brought about via a ring or a diagonal exchange interaction term in the effective Hamiltonian.

We further consider a second model in which the rung exchange interactions are described by the Ising-like Heisenberg Hamiltonian. In this case also, the spinon pair in a single chain is bound and the bound pair lowers its kinetic energy by hopping between chains. Kohno et al. [15] have studied a $S = \frac{1}{2}$ spatially anisotropic frustrated Heisenberg antiferromagnet in 2d in the weak interchain coupling regime. The model provides a good quantitative fit to the inelastic neutron scattering data of the triangular antiferromagnet Cs_2CuCl_4 . The spectrum consists of a continuum arising from the deconfinement of spinons in individual chains and a sharp dispersing peak associated with the coherent propagation of a triplon bound state of two spinons between neighbouring chains. In the case of our model, the bound pair has $S^z = +1$. One can similarly construct an $S^z = -1$ excitation. In summary, we have studied ladder models with the Ising-like Heisenberg Hamiltonian describing the interactions in individual chains. The rung interactions may be pure Ising or Ising-like Heisenberg. The ladder models studied in this paper share some common features with models in which the exchange interactions are isotropic. In the latter case, two types of models have generally been considered : ladder models in which the rung exchange interactions are the most dominant and models which describe spin chains coupled by weak exchange interactions. The models considered in this paper belong to a category not studied earlier and provide considerable physical insight on the origin of spinon confinement and how the bound spinon pairs delocalize. The isotropic models have, however, a richer dynamics with interactions generating cascades of virtual particles so that the two-body confinement problem becomes a many-body one [21]. The major common feature emerging from the study of ladder models with both Ising-like and isotropic exchange interactions appears to be the confinement of spinons in the form of bound states. The origin of excitation continua in specific cases lies in multi-triplon excitations rather than in the fractionalization of excitations [18].

References

- [1] H-J Mikeska and A. K. Kolezhuk in *Quantum Magnetism*, edited by U. Schollwöck, J. Richter, D. J. J. Farnell and R. F. Bishop (Springer, Berlin, 2004) p1
- [2] J. Richter, J. Schulenberg and A. Honecker in *Quantum Magnetism*, edited by U. Schollwöck, J. Richter, D. J. J. Farnell and R. F. Bishop (Springer, Berlin, 2004) p85
- [3] I. Bose, *Current Science* **88**, 62 (2005)
- [4] H. Bethe, *Z. Physik* **71**, 205 (1931)
- [5] B. Sutherland in *Beautiful Models* (World Scientific, Singapore)
- [6] J. Villain, *Physica B* **79**, 1 (1975)
- [7] N. Ishimura and H. Shiba, *Progs. Theor. Phys.* **63**, 743 (1980)
- [8] S. E. Nagler, W. J. L. Buyers, R. L. Armstrong and B. Briat, *Phys. Rev. B* **28**, 3873 (1983)
- [9] D. A. Tennant, T. G. Perring, R. A. Cowley and S. E. Nagler, *Phys. Rev. Lett.* **70**, 4003 (1993)
- [10] P. W. Anderson in *The Theory of Superconductivity in the High- T_c Cuprates* (Princeton University Press, Princeton, 1997)
- [11] S. A. Kivelson, D. S. Rokhsar and J. P. Sethna, *Phys. Rev. B* **35**, 8865 (1987)
- [12] M. Levin and T. Senthil, *Phys. Rev. B* **70**, 220403 (2004)
- [13] R. Coldea, D. A. Tennant, A. M. Tsvelik and Z. Tylczynski *Phys. Rev. Lett.* **86**, 1335 (2001)
- [14] R. Coldea, D. A. Tennant and Z. Tylczynski, *Phys. Rev. B* **68**, 134424 (2003)
- [15] M. Kohno, O. A. Starykh and L. Balents, *Nature Physics* **3**, 790 (2007)
- [16] D. G. Shelton, A. A. Nersisyan and A. M. Tsvelik, *Phys. Rev. B* **53**, 8521 (1996)
- [17] M. Greiter, *Phys. Rev. B* **66**, 054505 (2002)
- [18] C. Knetter, K. P. Schmidt, M. Grüninger and G. S. Uhrig *Phys. Rev. Lett.* **87**, 167204 (2001)
- [19] A. K. Kolezhuk and H-J Mikeska, *Int. J. Mod. Phys. B* **5**, 2305 (1998)
- [20] J. -B. Fouet, F. Mila, D. Clarke, H. Youk, O. Tchernyshyov, P. Fendley and R. M. Noack, *Phys. Rev. B* **73**, 214405 (2006)
- [21] B. Lake, A. M. Tsvelik, S. Notbohm, D. A. Tennant, T. G. Perring, M. Reehuis, C. Sekar, G. Krabbes and B. Büchner, *Nature Physics* **6**, 50-55 (2009)
- [22] F. Mila, *Eur. Phys. J. B* **6**, 201 (1998)
- [23] K. Tandon, S. Lal, S. K. Pati, S. Ramasesha and D. Sen, *Phys. Rev. B* **59**, 396 (1999)
- [24] N. Shannon, G. Misguich and K. Penc, *Phys. Rev. B* **69**, 220403(R) (2004)

- [25] L. Balents, M. P. A. Fisher and S. M. Girvin, Phys. Rev. B **65**, 224412 (2002)
- [26] I. Bose and S. Chatterjee Jour. Phys. C **16**, 947 (1983)
- [27] J. B. Torrance Jr. and M. Tinkham, Phys. Rev. **187**, 595 (1969)
- [28] T. Schneider and E. Stoll, Phys. Rev. Lett. **47**, 377 (1981)
- [29] C. K. Majumdar and D. K. Ghosh, J. Math. Phys. **10**, 1388 (1969)
- [30] F. D. M. Haldane Phys. Rev. Lett. **60**, 635 (1988)
- [31] B. S. Shastry, Phys. Rev. Lett. **60**, 639 (1988)
- [32] B. S. Shastry and B. Sutherland, phys. Rev. Lett. **47**, 964 (1981)
- [33] W. Zheng, C. J. Hamer, R. R. P. Singh, S. Trebst and H. Monien, Phys. Rev. B. **63**, 144411 (2001)